Pharmacokinetics and radiation dosimetry of ^{99m}Tc-3PRGD$_2$ in healthy individuals: A pilot study

CHENG Guanghui[1] GAO Shi[1] JI Tiefeng[1] MA Qingjie[1] JIA Bing[2]
CHEN Zuowei[3] WANG Qing[1,*]

[1]*China-Japan Union Hospital*, *Jilin University*, *Changchun 130033*, *China*

[2]*Medical Isotopes Research Center*, *Peking University*, *Beijing 100191*, *China*

[3]*Department of Nuclear Medicine*, *People's Hospital of Shenzhen*, *Shenzhen 518020*, *China*

Abstract ^{99m}Tc-3PRGD$_2$ is a new SPECT radiotracer for several tumor imaging with high uptake where integrin $\alpha_v\beta_3$ is highly expressed. This pilot study was to assess the safety, biodistribution and radiation dosimetry of ^{99m}Tc-3PRGD$_2$ in healthy volunteers. The 10 healthy male volunteers were injected with ^{99m}Tc-3PRGD$_2$ (786.7±55.8 MBq, 19.1–24.2 mCi). Baseline measurements of vital signs, laboratory safety tests and 12-lead electrocardiogram were recorded before and after injection. Blood and urine samples were collected and radiation counts were obtained at various time points. Whole-body scans and ROIs of identified organs were used for visual analysis and estimating the radiation dosimetry. No adverse reactions were found during the study. ^{99m}Tc-3PRGD$_2$ exhibited a rapid clearance from the blood with less than 45% of the initial dosage at 10 min after injection and gradual increasing radioactivity in urine with (52.9±6)% of original dose at 1440 min. The whole-body imaging showed high radioactive accumulation in bladder. And the highest ^{99m}Tc-3PRGD$_2$ uptake was found in the kidneys (3.50×10^{-2} mSv/MBq). The ^{99m}Tc-3PRGD$_2$ exhibited good pharmacokinetic properties and little radiation burden. This study showed that ^{99m}Tc-3PRGD$_2$ would be a safe and attractive SPECT agent in clinic applications.

Key words ^{99m}Tc-3PRGD$_2$, Integrin $\alpha_v\beta_3$, Pharmacokinetic, Dosimetry

1 Introduction

Cancer is a primary cause of death worldwide. There are about 7 million people died of cancer every year. Early diagnosis of cancer may lead to a higher rate of successful treatment and extend patient lives. So far, complicated factors were identified involving in the development of cancer. Angiogenesis, the formation of new blood vessels, has been considered as one of the key requirements for tumor initiation, growth, invasion and relapse[1,2]. It is generally accepted that solid tumor diameter rarely exceeds 2–3 mm without angiogenesis providing the nutrition to the tumor foci [3,4]. The process of new vessel formation is closely related to various factors including integrins. Integrins are a family of transmembrane glycoproteins consisting of different alpha and beta submits. They always play essential roles in cellular adhesion, migration and signal transduction. Among them, integrin $\alpha_v\beta_3$ is well examined due to its role in regulating angiogenesis[5]. It has been found to be highly expressed on the activated endothelial cells and the some tumor cells, but not the quiescent vessels and the normal cells[6,7]. Therefore, the targeting integrin $\alpha_v\beta_3$ in the angiogenesis may facilitate the early diagnosis of tumor foci and monitoring antiangiogenic treatment response.

Over the last decade, a series of arginine-glycine-aspartic acid (RGD) radiotracers which can specifically bind to the integrin $\alpha_v\beta_3$ have been considered as desirable imaging agents for non-

Supported by the National Natural Science Foundation of China (NSFC) projects (no.81271606) and the Research Fund of Science and Technology Department of Jilin Province (no. 201015185 and no. 201201041) and the Research Fund of Shenzhen Sci-tech Department of Guangdong Province (no.201102154).

* Corresponding author. *E-mail address:* wangqing@tom.com

Received date: 2012-06-05

invasively visualizing and quantifying the expression level of integrin $\alpha_v\beta_3$ by using some imaging modalities, such as positron emission tomography (PET) and single photon emission computed tomography (SPECT)[8−11]. Among these RGD-based radiotracers studied, the ^{18}F-AH111585 and ^{18}F-Galacto-RGD, 2 favorable PET agents, have been well investigated in both animal models and patients. The results showed that both radiotracers had high sensitivity for various types of tumors[12,13]. However, the high cost and lack of availability in developing countries limit the applications of PET imaging. SPECT is always an alternative method because of its low cost and easy preparation. And SPECT tracers usually have a longer half-life than those used for PET. ^{99m}Tc-NC100692, a ^{99m}Tc-labeled RGD-containing peptide was evaluated for detection of various cancers successfully for years[14,15]. A [^{99m}Tc (HYNIC-3PRGD$_2$) (tricine) (TPPTS)] (^{99m}Tc-3PRGD$_2$), a new ^{99m}Tc-labeled RGD dimeric peptide with PEG$_4$ linkers, has been reported as a SPECT radiotracer for tumor imaging in several xenograft models. It offered significant advantages of simple preparation, rapid clearance and high uptake in regions of neovascularization where the integrin $\alpha_v\beta_3$ is highly expressed[16,17].

Based on these favorable study results and our continuous interest in its proficiency of angiogenesis targeting, herein, we tentatively applied this new SPECT tracer in 10 healthy volunteers for the first time[18,19]. This pilot study was to assess the safety, biodistribution and radiation dosimetry of ^{99m}Tc-3PRGD$_2$ in the first healthy volunteers.

2 Material and Method

The protocol was approved by the institutional review board and independent ethic committees of China-Japan Union Hospital, Changchun, China. Written informed consent was obtained from all volunteer participants prior to the commencement of the study.

2.1 Radiopharmaceutical Preparation

The 3PRGD$_2$ kit was generously provided by Medical isotopes research center of Peking University containing per mL, 20 μg of HYNIC-3PRGD$_2$, 5 mg of TPPTS, 6.5 mg of tricine, 40 mg of mannitol, 38.5 mg of disodium succinate hexahydrate, and 12.7 mg of succinic acid. 1–1.5 mL of Na^{99m}TcO$_4$ solution (1 110 –1 850 MBq) in saline was added into each kit vial followed by the incubation of 20–25 min at 100°C. Then the vial was placed back into the lead pig and allowed to stand at room temperature.

A quality control by radioactive instant thin-layer chromatography (radio-ITLC) and radioactive high-performance liquid chromatography (radio-HPLC) were performed before injection of the agent. A radio-chemical purity (RCP) of greater than 95% was required in this study.

2.2 Subjects

The healthy volunteer population consisted of 10 healthy male volunteers aged between 27 and 53 years. The height, weight and body mass index of the subjects were 175.4±5.8 cm, 68.2±5.3 kg and 22.9±1.0 kg/m^2, respectively (Table 1). Physical examination and laboratory results from last 6 months demonstrated no pathologic findings for all volunteers.

Table 1 Subject baseline characteristics and RGD dose data.

Volunteer No/Sex/Age(y)	Height (cm)	Weight (kg)	Body mass index (kg/m^2)	Injected Activity (MBq)
1/M/27	175.3	62.1	23.5	800.3
2/M/31	169.5	69.2	24.1	768.1
3/M/33	180.1	77.4	23.9	859.1
4/M/45	170.6	65.9	22.6	731.5
5/M/53	185.8	80.7	23.3	895.8
6/M/41	172.6	61.8	20.7	763.9
7/M/39	177.9	70.3	22.2	780.3
8/M/47	170.0	69.6	24.1	772.6
9/M/33	183.2	61.1	23.7	789.2
10/M/50	172.4	63.6	21.3	706.0

2.3 Assessments and Sample Collection

The ^{99m}Tc-3PRGD$_2$ with a range of 786.7±55.8 MBq (19.1–24.2 mCi) was injected into the antecubital vein with a rapid bolus, followed by a 10 mL saline flush. Measurements of vital signs (body temperature, systolic and diastolic blood pressure and pulse rate), laboratory safety tests (renal and liver function chemistry, hematology, and blood coagulation parameters) and 12-lead electrocardiogram were recorded before and after tracer injection.

The 1.5 mL blood sample was collected via an indwelling catheter throughout the imaging period specifically at 2-, 3-, 5-, 10-, 15-, 30- and 60-min post-injection. Samples were weighed and counted in a γ-counter (Wallac 1470-002, Perkin Elmer, Finland). Decay corrected time-activity curve was expressed as percentage of injected dose per gram (%ID/g).

After tracer injection, urine sample was collected at the intervals of 0–120, 120–240, 240– 480, 480–720 and 720–1440 min. Samples were weighed and radioactivity was measured with the γ-counter.

Any unusual or adverse symptoms were recorded during the study based on vital signs, hematologic values and ECGs.

2.4 SPECT Procedure

Whole-body scans were performed via a SPECT scanner (Philips Healthcare) equipped with parallel-hole, low-energy and high-resolution collimators. All images were acquired using the ^{99m}Tc with a 20% energy window centered on 140 keV. Both anterior and posterior images were acquired at 10-, 30-, 60-, 120-, and 240-min post-injection and were stored digitally in a 256 × 256 matrix. The velocity of scanning was 15 cm/min.

2.5 Biodistribution and Dosimetry Estimation

Visual analysis was applied to determine the integral biodistribution of the tracer and transient and intersubject stability. For each subject, regions of interest (ROIs) were delineated over the identified organs including: lung, heart, liver, kidneys, spleen, intestine, urinary bladder, and a background region near the body on the anterior image. The mirror ROIs were applied to the posterior images of each organ. The mean counts of each organ including anterior and posterior images were measured. The results were expressed as percentage of initial injected activity after decay-correction.

Fitted residence time functions were plotted and multiplied by the exponential decay functions for ^{99m}Tc. These functions were then integrated analytically to determine the area under the curve (AUC) to yield the residence time of each organ. Then, these residence time were input in OLINDA/EXM 1.0 software (Vanderbilt, University, Nashville, TN) to calculate equivalent organ doses and the effective dose (ED) based on the 70-kg reference adult phantom in International Commission on Radiological Protection (ICRP) publication 60[20].

3 Results

No clinically significant abnormalities or abnormal clinical chemistry were reported by the volunteers during the study.

Figure 1 shows a representation of a coronal section from whole-body SPECT and the distribution of ^{99m}Tc-3PRGD$_2$ at 10-, 30-, 60-, 120-, and 240-min post-injection. The predominant uptake was seen in the bladder, indicating a renal-urinary excretion of the tracer. The kidneys and liver showed moderate uptake. Apparent tracer uptake was observed in nasal cavity, salivary glands and the thyroid in the early time points and almost undetectable after 240-min injection.

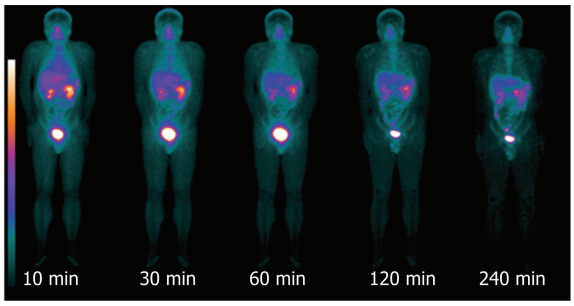

Fig.1 Series of coronal whole-body images of a representative subject showing the distribution of ^{99m}Tc-3PRGD$_2$ between 10 and 240-min post-injection.

By measuring ROIs drawn on both anterior and posterior images, the quantitative tracer uptakes in major organs were presented in Fig.2, the highest activity in visceral organs was found in the bladder which ascended from 13.95±3.91% ID/organ (10 min

p.i.) to 26.15±5.84% ID/organ (60 min p.i.). It was followed by the kidneys and the liver which declined over time (10 min p.i. to 60 min p.i, 10.22±1.89% to 6.89±1.24% ID/organ, and 7.85±1.07% to 5.97% ±1.81% ID/organ, respectively). Low activities were remained in the intestines, spleen, lungs and heart till 60 min after injection (2.20±0.98%, 1.46±0.32%, 1.42 ±0.10%, 1.07±0.20% ID/organ, respectively).

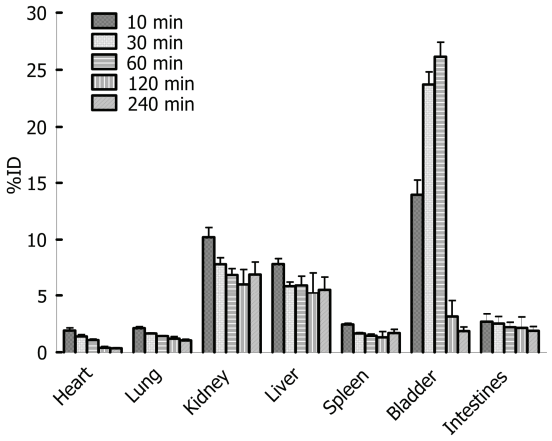

Fig.2 The quantified analysis of ^{99m}Tc-3PRGD$_2$ in major organs of healthy volunteers from the whole-body images at 10, 30, 60, 120 and 240 min after administration.

Fig.3 gives the time-activity curve reporting the blood clearance over the first 60 min. The data showed there was a very sharp decline of radioactivity in the circulation with less than 45%, 18% and 12% of the initial dosage at 10, 30 and 60 min respectively after injection.

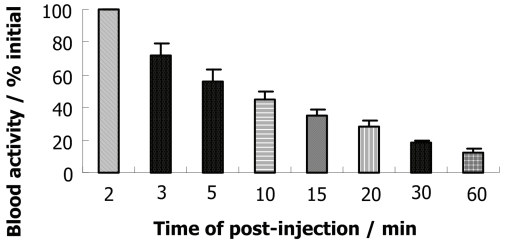

Fig.3 Averaged time-activity curve of ^{99m}Tc-3PRGD$_2$ in blood for all healthy volunteers. Error bars indicate standard deviations.

The concentration of radioactivity in urine was shown in Fig.4. The radioactivities in urine keep increasing with a total cumulative recovery of (52.9± 6) % of original dose at 1440 min. ~50% of the tracer remained in the circulation at (1960±156) min.

A summary of dosimetric parameters for various organs and whole body is given in Table 2. Among them, the kidneys received the highest absorption (3.50×10^{-2} mSv/MBq) because of the dominant excretion of ^{99m}Tc-3PRGD$_2$ via renal pathway. The brain, breast, testis and skin showed the relative low uptake of ^{99m}Tc-3PRGD$_2$ (7.33×10^{-4}, 1.81×10^{-3}, 2.03×10^{-3}, and 1.59×10^{-3} mSv/MBq). Although only men were involved in our study, OLINDA/EXM 1.0 software also gives an estimate of the dose in ovaries if these had been present (3.11×10^{-3} mSv/MBq). The mean effective dose equivalent of whole body was 3.92×10^{-3} mSv/ MBq.

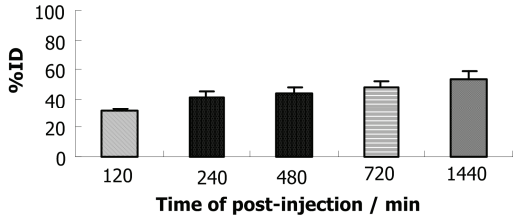

Fig.4 Averaged time-activity curve of ^{99m}Tc-3PRGD$_2$ in urine for all healthy volunteers. Error bars indicate standard deviations.

4 Discussion

^{99m}Tc-3PRGD$_2$ was first described in 2009 and was further verified as an integrin $\alpha_v\beta_3$ imaging agent in following studies[16,18,21,22]. However, the associated radiation burden in normal human has not been studied. The purpose of this study was to verify whether ^{99m}Tc-3PRGD$_2$ is a safe and stable tracer for potential clinical application.

The absence of adverse effects on vital signs after intravenous injection demonstrated the ^{99m}Tc-3PRGD$_2$ is safe. The rapid clearance from the blood with a half-life time less than 10 min and continuous accumulation in urine reflected the favorable pharmacokinetic properties of ^{99m}Tc-3PRGD$_2$.

According to the biodistribution of ^{99m}Tc-3PRGD$_2$, high bladder and kidneys uptake revealed the renal clearance of ^{99m}Tc-3PRGD$_2$, which is a pattern of excretion similar to that in healthy cynomolgus models[17] with a little metabolin in urine. The radioactivity accumulation in the liver indicated that ^{99m}Tc-3PRGD$_2$ was slightly metabolized *via* hepatobiliary system. And the accumulation in the liver, spleen, gallbladder, kidneys and urinary bladder may result in the blurry imaging of abnormal. On the other hand, lower uptakes of ^{99m}Tc-3PRGD$_2$ in

background tissues, especially heart, lungs and brain would be an advantage for high-quality images and reliable quantification. These results were accordance with the previous studies in which ^{99m}Tc-3PRGD$_2$ had been confirmed as an excellent radiotracer in visualization of MDA-MB-435 tumor in mouse xenograft models[21].

Table 2 Dosimetric data of ^{99m}Tc-3PRGD$_2$ (n=10).

Target Organ	mSv/MBq（Mean ±*SD*）	Rem/mCi (Mean ±*SD*)
Adrenal glands	$(5.39\pm0.46)\times10^{-3}$	$(2.00\pm0.17)\times10^{-2}$
Brain	$(7.33\pm0.80)\times10^{-4}$	$(2.71\pm0.29)\times10^{-3}$
Breast	$(1.81\pm0.15)\times10^{-3}$	$(6.70\pm0.56)\times10^{-3}$
Gallbladder wall	$(5.43\pm0.11)\times10^{-3}$	$(2.01\pm0.04)\times10^{-2}$
Lower region of colon	$(2.91\pm0.71)\times10^{-3}$	$(1.08\pm0.26)\times10^{-2}$
Small intestine	$(3.55\pm0.21)\times10^{-3}$	$(1.31\pm0.08)\times10^{-2}$
Stomach wall	$(3.80\pm0.10)\times10^{-3}$	$(1.40\pm0.04)\times10^{-2}$
Upper colon	$(3.58\pm0.10)\times10^{-3}$	$(1.33\pm0.04)\times10^{-2}$
Heart wall	$(3.94\pm0.28)\times10^{-3}$	$(1.46\pm0.10)\times10^{-2}$
Kidneys	$(3.50\pm0.29)\times10^{-2}$	$(1.30\pm0.11)\times10^{-1}$
Liver	$(8.35\pm0.37)\times10^{-3}$	$(3.09\pm0.14)\times10^{-2}$
Lungs	$(3.58\pm0.43)\times10^{-3}$	$(1.32\pm0.16)\times10^{-2}$
Muscle	$(2.49\pm0.23)\times10^{-3}$	$(9.22\pm0.85)\times10^{-3}$
Ovaries	$(3.11\pm0.22)\times10^{-3}$	$(1.15\pm0.08)\times10^{-2}$
Pancreas	$(5.38\pm0.16)\times10^{-3}$	$(1.99\pm0.06)\times10^{-2}$
Red marrow	$(2.71\pm0.03)\times10^{-3}$	$(1.00\pm0.01)\times10^{-2}$
Osteogenic cells	$(6.67\pm0.29)\times10^{-3}$	$(2.47\pm0.11)\times10^{-2}$
Skin	$(1.59\pm0.07)\times10^{-3}$	$(5.90\pm0.26)\times10^{-3}$
Spleen	$(1.63\pm0.25)\times10^{-2}$	$(6.04\pm0.93)\times10^{-2}$
Testis	$(2.03\pm0.04)\times10^{-3}$	$(7.52\pm0.15)\times10^{-3}$
Thymus	$(2.54\pm0.19)\times10^{-3}$	$(9.39\pm0.70)\times10^{-3}$
Thyroid gland	$(9.04\pm0.96)\times10^{-3}$	$(3.35\pm0.36)\times10^{-2}$
Urinary bladder wall	$(2.71\pm0.16)\times10^{-3}$	$(1.00\pm0.06)\times10^{-2}$
Uterus	$(3.11\pm0.15)\times10^{-3}$	$(1.15\pm0.06)\times10^{-2}$
Whole body	$(2.94\pm0.09)\times10^{-3}$	$(1.09\pm0.03)\times10^{-2}$
Effective dose equivalent	$(6.51\pm0.23)\times10^{-3}$	$(2.41\pm0.09)\times10^{-2}$
Effective dose	$(3.92\pm0.21)\times10^{-3}$	$(1.45\pm0.08)\times10^{-2}$

According to the guidelines set forth by the 2007 International Commission on Radiological Protection[23,24], the radiation dose limit for critical organ is 500 mSv (50 rem) and that for radiation-sensitive organs (such as the testes and ovaries) is 150 mSv (15 rem) per year. In this study, the kidneys showed the highest uptake of ^{99m}Tc-3PRGD$_2$ and about 786.7 MBq of ^{99m}Tc-3PRGD$_2$ injected led to an effective dose equivalent of ~3.50×10^{-2} mSv/MBq. Other major organs showed lower uptake and the mean absorbed radiation dose of entire body was 3.92×10^{-3} mSv/MBq. According to the reference 70-kg adult man and 11.1 MBq/kg dose, an effective dose of 3.08 mSv (0.308 rem) would be absorbed for one diagnostic study. This value is lower than ^{99m}Tc-MIBI myocardial imaging (7.05 mSv, 0.705 rem) or ^{99m}Tc-MDP bone scan (5.92 mSv, 0.592 rem)[25], which would facilitate longitudinal scans of the same subject.

The primary disadvantage of this study was that only 10 healthy volunteers were involved. This limited the statistical analyses in particular. Again, the pharmacokinetics and dosimetry including these assessments in patients were not further performed.

5 Conclusions

No adverse reactions were observed during this study. ^{99m}Tc-3PRGD$_2$ exhibited a rapid clearance from the blood largely by the kidneys. The effective radiation dose is significantly lower than the limit value according to ICRP 60, showing an acceptable radiation burden. Our findings indicated that ^{99m}Tc-3PRGD$_2$ would be a safe SPECT agent in clinic applications.

References

1 Folkman J. Cancer Med, 2000, 132–52.

2 Folkman J. Semin Oncol, 2002, **29(6 Suppl 16):** 15–18.

3 Jain R K, Munn L L, Fukumura D. Nat Rev Cancer, 2002, **2:** 266–76.
4 Brown E B, Campbell R B, Tsuzuki Y, *et al.* Nat Med, 2001, **7:** 864–868.
5 Hynes R O. Cell, 1987, **48:** 549–554.
6 Horton M A. Int J Biochem Cell Biol, 1997, **29:** 721–725.
7 Plow E F, Haas T A, Zhang L, *et al.* J Biol Chem, 2000, **275:** 21785–21788.
8 Ruoslahti E, Pierschbacher M D. Sci, 1987, **238:** 491–497.
9 Haubner R, Weber W A, Beer A J, *et al.* PLoS Med, 2005, **2:** e70.
10 Beer A J, Haubner R, Goebel M, *et al.* J Nucl Med, 2005, **46:** 1333–1341.
11 Indrevoll B, Kindberg G M, Solbackken M, *et al.* Bioorg Med Chem Lett, 2006, **16:** 6190–6193.
12 Beer A J, Haubner R, Sarbia M, *et al.* Clin Cancer Res, 2006, **12:** 3942–3949.
13 Kenny L M, Coombes R C, Oulie I, *et al.* J Nucl Med, 2008, **49:** 879–886.
14 Bach-Gansmo T, Danieleeon R, Saracco A, *et al.* J Nucl Med, 2006, **47:** 1434–1439.
15 Axelsson R, Bach-Gansmo T, Castell-Conesa J, *et al.* Acta Radiol, 2010, **51:** 40–46.
16 Wang L, Shi J, Kim Y S, *et al.* Mol Pharm, 2009, Jan-Fed, **6:** 231–245.
17 Jia B, Liu Z, Zhu Z, *et al.* Mol Imaging Biol, 2011, **13:** 730–736.
18 Ma Q, Ji B, Jia B, *et al.* Eur J Nucl Med Mol Imaging, 2011, **38:** 2145–2152.
19 Zhu Z, Miao W, Li Q, *et al.* J Nucl Med, 2012, **53:** 1–7.
20 International commission on radiological protection. Recommendations of the international commission on radiological protection. Publication 60. Oxford, England: Pergamon Press,1991.
21 Zhou Y, Kim Y S, Chakraborty S, *et al.* Mol Imaging, 2011, **10:** 386–397.
22 Shi J, Wang L, Kim Y S, *et al.* J Med Chem, 2008, **51:** 7980–7990.
23 International commission on radiological protection. Radiation protection in medicine. ICRP publication 105. Ann ICRP 2007, **37:** 1–63.
24 International commission on radiological protection. The 2007 recommendations of the international commission on radiological protection. ICRP publication 103. Ann ICRP 2007, **37:** 1–332.
25 Kubo A, Nakamura K, Sanmiya T, *et al.* Kaku lgaku, 1991, **28:** 1133–1142.